Bioelectrochemistry 147 (2022) 108216

Contents lists available at ScienceDirect

Bioelectrochemistry

journal homepage: www.journals.elsevier.com/bioelectrochemistry

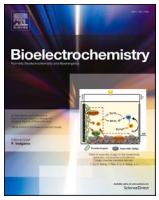

Models of electroporation and the associated transmembrane molecular transport should be revisited

Maria Scuderi [a], Janja Dermol-Černe [a], Clarissa Amaral da Silva [b], Aswin Muralidharan [b], Pouyan E. Boukany [b], Lea Rems [a,*]

[a] University of Ljubljana, Faculty of Electrical Engineering, Tržaška cesta 25, SI-1000 Ljubljana, Slovenia
[b] Delft University of Technology, Department of Chemical Engineering, Van der Maasweg 9, 2629 HZ Delft, The Netherlands

ARTICLE INFO

Keywords:
Electropermeabilization
Mathematical modeling
Electrodiffusion
Molecular transport
Multiphysics
Multiscale

ABSTRACT

Electroporation has become a powerful tool for nonviral delivery of various biomolecules such as nucleic acids, proteins, and chemotherapeutic drugs to virtually any living cell by exposing the cell membrane to an intense pulsed electric field. Different multiphysics and multiscale models have been developed to describe the phenomenon of electroporation and predict molecular transport through the electroporated membrane. In this paper, we critically examine the existing mechanistic, single-cell models which allow spatially and temporally resolved numerical simulations of electroporation-induced transmembrane transport of small molecules by confronting them with different experimental measurements. Furthermore, we assess whether any of the proposed models is universal enough to describe the associated transmembrane transport in general for all the different pulse parameters and small molecules used in electroporation applications. We show that none of the tested models can be universally applied to the full range of experimental measurements. Even more importantly, we show that none of the models has been compared to sufficient amount of experimental data to confirm the model validity. Finally, we provide guidelines and recommendations on how to design and report experiments that can be used to validate an electroporation model and how to improve the development of mechanistic models.

1. Introduction

The theoretical basis for phenomena observed when biological cells are exposed to external electric fields has made important contributions in biomedicine, ranging from electric-field-based cell manipulation and cell sorting [1,2] to non-viral gene and drug delivery [3,4]. Early studies from the beginning of the 20th century found that from an electrical point of view, a cell can be viewed as a conducting body (the cytoplasm) surrounded by a thin dielectric sheath (the cell membrane) [5]. Thus, when an external electric field is applied to a cell, an induced transmembrane voltage (TMV) is formed across its membrane, which varies with position on the membrane and increases linearly with the strength of the applied electric field [6,7]. When the TMV exceeds a certain critical absolute value (typically reported on the order of several 100 mV), it causes structural changes in the cell membrane that increase its permeability and conductivity. The phenomenon is called electroporation (also electropermeabilization) and allows the influx and efflux of ions and molecules that otherwise cannot readily pass through the cell membrane.

Once the cell membrane is electroporated, the mechanisms contributing to the transmembrane transport are diffusion, electrophoresis, electroosmosis, and endocytosis [6,8–10]. Diffusive transport is due to a concentration gradient between the intracellular and extracellular sides of the membrane. Electrophoretic transport is due to the Coulomb force exerted on charged particles by the local electric field. Electroosmotic transport is the motion of intracellular and/or extracellular fluid (water and solutes) through pores in the membrane, which is induced by an electric field acting on charged ions at the membrane-water interface. Endocytosis is a process in which particles are internalized through an area of the cell membrane that forms a vesicle. During pulse application, transport is mainly electrophoretic and possibly electroosmotic [9,11–13]. After pulse application, when no external electric field is present, the transport is governed by a combination of diffusion, electrophoresis driven by the intrinsic (resting)

* Corresponding author.
E-mail address: lea.rems@fe.uni-lj.si (L. Rems).

https://doi.org/10.1016/j.bioelechem.2022.108216
Received 7 June 2022; Received in revised form 19 July 2022; Accepted 20 July 2022
Available online 25 July 2022

membrane voltage, and in some cases endocytosis [8,13,14]. The transport mechanisms that contribute most to the total amount of transported molecules depend on the pulse duration and/or amplitude, the charge and size of the molecule, and the time taken for the membrane to recover to its impermeable state (resealing time) [8,15]. A visual schematic of the process of electroporation and the associated molecular transport is presented in Fig. 1.

Electroporation is used for enhancing transmembrane transport in a broad range of applications, including medicine (e.g., electrochemotherapy, gene electrotransfer, transdermal drug delivery) [3], biotechnology [16], food technology [17], and environmental science [18,19]. The parameters of electric pulses used in these applications vary greatly, largely as a consequence of historical development and the availability of pulse generators, but also because certain pulse waveforms have been found better suited for specific applications [8,20–22]. Nowadays, the pulse durations span 9 orders of magnitude from hundreds of picoseconds to hundreds of milliseconds, and electric field amplitudes achieved during the applied pulses span 3 orders of magnitude from hundreds of V/cm to hundreds of kV/cm. The electric field can be delivered in the form of individual electric pulses or bursts of pulses. The pulses can be monopolar or bipolar. The pulse shape can be rectangular, triangular, sinusoidal, or exponentially decaying. The number of pulses can vary from a single pulse to hundreds of pulses [3,23]. For each electroporation application, which aims to achieve transport of a sufficient amount of molecules through the membrane under conditions of reversible electroporation (cells survive), the pulse parameters must be carefully optimized. This optimization process is time-consuming, costly, and labor-intensive as it is based only on trial-and-error experimentation. In this context, models of electroporation can become an excellent tool to study the response of cells to different pulse parameters in various experimental configurations.

Scientists have developed different multiphysics and multiscale models which allow spatially and temporally resolved numerical simulations of electroporation and molecular transport through the electroporated membrane at the single-cell level. Many of these models have been compared qualitatively and/or quantitatively with experimental measurements of small molecule uptake into cells, as well as other measurements, such as an increase in membrane conductivity or time courses of the induced TMV [24–27]. Curiously, despite their differences, models containing different theoretical descriptions of electroporation and transmembrane molecular transport have generally reported good agreement with experimental results. Obviously, all these different models cannot simultaneously be valid. Is the electroporative molecular transport so insensitive to the details in the physical description of the electroporation process, or is there a general problem in how the models are developed and validated? In this paper, we investigate whether any of the existing single-cell models can be considered validated. Furthermore, we critically examine whether any of these models is universal enough to describe electroporation and associated molecular transport in general for all the different pulse parameters used in electroporation applications. To this end, we provide an overview of existing mathematical models of electroporation-induced transmembrane transport of small molecules at the level of single animal cells. We divide the models into three groups based on how they theoretically describe the increase in membrane permeability: (i) pore states models; (ii) pore distribution models; (iii) other phenomenological models, and we select three representative models from the first two groups. We implement the selected models and compare them to a set of previously published experimental measurements of small molecule uptake obtained with a wide range of pulse parameters. In particular, we focus on comparing the models with experimental results to which the models were not compared in their original publications. Using various examples, we show that none of the tested models can be universally applied to the full range of experimental measurements. Importantly, we show that none of the models has been confronted with sufficient amount of experimental data to confirm the model validity. Finally, we provide guidelines/recommendations on how to design experiments to validate an electroporation model, as well as how to improve the development of mechanistic models.

2. Literature survey

To identify models that describe the phenomenon of electroporation and the transport of small molecules through the electroporated membrane we began our study with a literature survey. We used the research platform Web of Science using the keywords: electroporation OR electropermeabili*ation **AND** mathematical OR numerical **AND** model OR simulation **AND** transport and searched for papers that were published up to the end of 2021. The search returned 91 papers. By assessing the content of all 91 papers (based on title, abstract, and additional information in the manuscripts), we selected 6 relevant papers

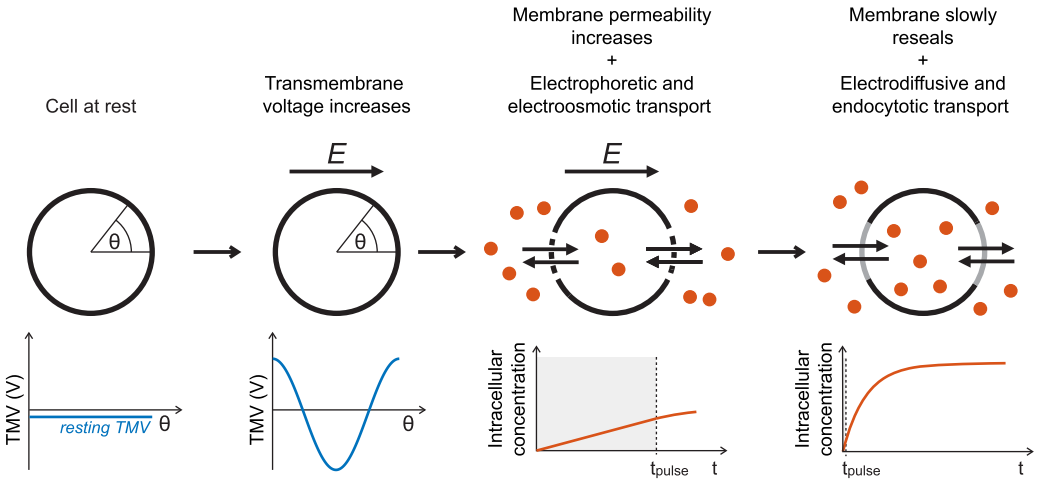

Fig. 1. The process of cell electroporation and the associated transmembrane molecular transport. Exposure to an electric field induces a TMV that varies with position on the membrane. In the regions, where the TMV exceeds a certain threshold (reported on the order of several 100 mV), enhanced transmembrane transport of ions and molecules is observed. Transmembrane transport is bidirectional; the red dots in the figure shows only the molecular uptake into the cell. During the pulse, the transport is primarily electrophoretic and possibly electroosmotic, whereas after the pulse the transport is electrodiffusive and in some cases endocytotic. After exposure to an electric field, the transmembrane molar flux decreases with time due to cell membrane resealing.

[12,29,36,38,41,48] that met our first criterium: 1) The model describes electroporation-mediated uptake of ions or small molecules in animal cells at the single-cell level. We limited our study to models describing the transport of small molecules, since, in the case of large molecules like DNA, the transport mechanisms are considerably more complex, less understood, and thus also less addressed by theoretical studies [8,28]. We also decided to exclude studies on plant and bacterial cells, not to include the cell wall as a confounding factor. In addition, most of the quantitative measurements of molecular uptake have been carried out in animal cells. We then searched for additional papers meeting criterium 1) by looking through the titles and abstracts of the cited and citing references of the selected 6 papers, which yielded 23 papers in total (Table 1). Based on the theoretical approach describing the increase in membrane permeability we divided the models into three groups: (i) pore states models; (ii) pore distribution models; (iii) other phenomenological models. The first two groups attribute the increase in membrane permeability specifically to the creation of pores in the lipid domains of the cell membrane under the influence of the induced TMV. The pore states models are based on a kinetic scheme that describes the transition between distinct states of pores created in the cell membrane. The pore distribution models describe pores created in the membrane by a distribution function defined in a pore radius space, whereby the pore size can change to minimize the membrane free energy. The third group corresponds to other phenomenological models, which generally do not make specific assumptions on the molecular mechanisms of the increase in membrane permeability but describe the latter using a strong phenomenological component. We then assessed the models using additional criteria: 2) The model enables numerical simulations of the spatially-resolved time course of electroporation-mediated molecular transport. 3) The model is mechanistic, i.e., it needs to include the proposed mechanisms of electroporation and transport at the single-cell level that can be traced back to the molecular nature of the structural changes in the cell membrane. We focused on mechanistic instead of phenomenological models, as mechanistic models have the potential to be universally applied to different experimental conditions, provided that they correctly capture the physical mechanisms of electroporation

Table 1
Papers describing models of electroporation and molecular transport and meeting criterium 1). Highlighted bold are papers that meet all criteria.

Model group	Authors	Year	Spatio-temporal	Mechanistic	Comparison with experiment	No. cit.**
Pore states models	Neumann et al. [25]	1998	no	yes	Quantitative comparison with the percentage of mouse B cells stained with Serva Blue G dye [25]	175
	Schmeer et al. [24]	2004	no	yes	Quantitative comparison with measurements of the changes in the conductivity of CHO cell pellets due to transport of monovalent ions [24]	82
	Miklavcic and Towhidi [29]	**2010**	yes	yes	Qualitative comparison with lucifer yellow uptake in DC3F hamster fibroblasts at a fixed time point induced by pulses of different shapes [32]	76
Pore distribution models	**Li and Lin** [12]	**2011**	yes	yes	Qualitative comparison with 2D profiles of calcium uptake measured in single CHO cells [33]	97
	Li et al. [30]	**2013**	yes	yes	Qualitative comparison with the percentage of electroporated Sp2 mouse myeloma cells stained with propidium iodide [34]	61
	Sadik et al. [35]	**2014**	yes	yes	Qualitative comparison with the total amount of fluorescein-dextran uptake in NIH-3T3 mouse fibroblasts induced by a double-pulse protocol [35]	36
	Mahboubi et al. [36]	2017	yes	yes	no	2
	Shil et al. [37]	2018	yes*	yes	no	3
	Goldberg et al. [38]	**2018**	yes	yes	Qualitative comparison with 2D profiles of calcium uptake measured in single CHO cells [33] Quantitative comparison with electrodeformation measured in erythrocytes [39] and GUVs [40]	32
	Goldberg et al. [41]	**2021**	yes	yes	Quantitative comparison with cisplatin uptake in B16F1 mouse melanoma cells at a fixed time point induced by different numbers of 100 us pulses [42]	3
	Yan et al. [43]	2021	yes	yes	no	2
	Guo et al. [44]	2021	yes	yes	no	2
	Smith [31]	**2011**	yes	yes	Quantitative comparison with lucifer yellow uptake in DC3F hamster fibroblasts and calcein uptake in DU 145 prostate cancer cells at a fixed time point induced by single pulses of different shape, duration and amplitude [10,45]	25
	Son et al. [46]	2014	yes	yes	no	91
	Son et al. [47]	2016	yes	yes	no	31
	Mi et al. [48]	2019	yes	yes	no	14
	Mi et al. [49]	**2021**	yes	yes	Qualitative and quantitative comparison with the time course of propidium iodide uptake in A375 human melanoma cells [49]	1
Other phenomenological models	Puc et al. [10]	2003	no	no	Quantitative comparison with lucifer yellow uptake in DC3F hamster fibroblasts at a fixed time point induced by 100 μs and 1 ms pulses of different amplitude [10].	153
	Pavlin et al. [50]	2007	no	no	Quantitative comparison with measurements of the changes in the	101
	Pavlin et al. [51]	2008	no	no	conductivity of dense suspensions of B16F1 mouse melanoma cells due to transport of monovalent ions [50]	120
	Leguebe et al. [52]	2014	yes	no	Qualitative comparison with 2D profiles of propidium iodide uptake in CHO cells and Jurkat T lymphocytes [53,54]. Qualitative interpretation of the effect of pulse repetition frequency on molecular uptake in potato tissue and mouse liver [55]	75
	Dermol et al. [42]	2018	no	no	Quantitative comparison with cisplatin uptake in B16F1 mouse melanoma cells at a fixed time point induced by different numbers of 100 μs pulses [42]	10
	Sweeney et al. [56]	2018	no	no	Quantitative comparison with the time course of propidium iodide uptake in CHO cells [57]	13

*The spatiotemporal resolution was limited since the cell was divided into 8 segments only.
**The number of citations for the given paper on July 18, 2022, according to Google Scholar. Note that some of the papers [10,24,25,35,42,49–51] report also original experimental measurements and are not necessarily cited for the developed model.

and transmembrane transport. 4) The model has been compared to quantitative, or at least qualitative experimental data.

All of our criteria were met by eight models (Table 1, highlighted bold), from which we selected three representatives for further testing: Miklavčič and Towhidi [29], Li et al. [12,30], and Smith [31] models. For brevity, we refer to these models as the MT2010 [29], LL2011 [12,30], and S2011 [31]. The MT2010 was chosen as the only model from the group of pore state models meeting all our criteria. The S2011 and LL2011 from the group of pore distribution models were selected because they formed the basis for all other published models. Moreover, S2011 and LL2011 models are hypothesized to be relatively universal, as they have already been used to simulate the uptake of different ions and molecules over a wide range of pulse parameters and experimental conditions (Table 2). Subsections 2.1–2.3 briefly describe the models from each of the groups, with emphasis on the MT2010, S2011, and LL2011 models. Table 2 shows, for each of the three selected models, the range of pulse parameters, for which the model was designed; the molecules, which were used to optimize/validate the model; the proposed dominant transport mechanism; and how the optimization/validation of the model was performed. As listing all equations behind each model is extremely lengthy, we focus in the main paper on the model aspects, which are important to understand the differences between individual models and their effect on the results presented in the paper. Full details of the models together with their numerical implementation are provided in Supplementary Information. All models used in this study are also available at https://github.com/learems/EPmodels-Electroporation-MolTransport.

2.1. Pore states models

A kinetic scheme describes the rate of chemical reactions or transitions between distinct states as a step-by-step sequence. Pore states models are based on the kinetic scheme which describes the transitions of the cell membrane: from the initial state when the cell membrane is intact, to the porous state when a sufficiently high electric field is applied, and back to the initial state when there is no electric field applied.

The first electroporation model based on a kinetic scheme was proposed by Neumann et al. in 1989 [58]. In 1998 the model was upgraded from one porous state [58] to three porous states to account for a second-order membrane resealing process observed experimentally [25]. Later on, Schmeer et al. [24] revised the model and proposed that there are two closed states (C and C_1) and two porous states (P_1 and P_2).

$$C \underset{k_{-1}}{\overset{k_1}{\rightleftarrows}} C_1 \underset{k_{-2}}{\overset{k_2}{\rightleftarrows}} P_1 \underset{k_{-3}}{\overset{k_3}{\rightleftarrows}} P_2 \tag{1}$$

where C is the intact membrane and C_1 is the stage in which membrane lipids reorganize tilting their headgroups. States P_1 and P_2 correspond to the formation of prepores and final pores, respectively, whereby only pores P_2 mediate the transmembrane transport of molecules. Molecular dynamics simulations of lipid bilayer electroporation corroborated the four-state model [59]. The forwards rates k_i ($i = 1, 2, 3$) in eq. (1) depend exponentially on the transmembrane voltage (TMV), whereas the backward rates k_{-i} are constant and independent of the TMV. Schmeer et al. [24] fitted the proposed model to the measurements of the change in the conductivity of Chinese hamster ovary (CHO) cell pellets. Unfortunately, their model cannot be reconstructed completely, as they did not report the values of all parameters, specifically the values of the backward rates.

The models described in [24,25,58] were based on analytical approaches for obtaining a solution to a system of equations, which require many simplifying assumptions and are only suitable for spherical cells. Furthermore, the distribution of pores in the electroporated regions at which the transport took place was assumed uniform, and the dynamic behavior of other parameters such as TMV and membrane conductivity and permeability was not considered. Miklavčič and Towhidi [29] solved these shortcomings by performing numerical simulations of electroporation and associated molecular transport in whole cells using a finite-element approach. They built upon the earlier models [24,25,58] and added a description for long-term diffusive and endocytic-like molecular uptake [29]. The model was in qualitative agreement with measurements of lucifer yellow uptake induced by pulses of different shapes [32]. The MT2010 model is the only one based on the kinetic scheme that enables simulations of the entire spatiotemporal dynamics of the electroporation and molecular transport process; therefore, it was chosen for testing in our study.

The MT2010 model describes the electroporation dynamics with eq. (1) following previous models. Similarly, as in previous models [24,25,58], the forward rates depend exponentially on TMV. The

Table 2
Models selected for further testing. For each model, the table reports the range of pulse parameters and the molecules, for which the model was designed (and which were used to optimize/validate the model); the proposed dominant transport mechanism, and how the modeling results were compared to experimental measurements.

		Pulse parameters	Molecules	Transport mechanism	Comparison with experiment
Pore states model	**MT2010 model** [29]	Electric field: 1 kV/cm No. pulses: 1 and 8 Pulse shape: unipolar/bipolar rectangular, triangular, sinusoidal, sinusoidal modulated rectangular pulses with 10 % and 90 % modulation Pulse duration: 1 ms Pulse rise time: 2 μs, 10 μs,100 μs Pulse repetition rate: 1 Hz	lucifer yellow	diffusion and endocytosis	Qualitative comparison with lucifer yellow uptake into DC3F spontaneously transformed Chinese hamster fibroblasts [32]. Cells were electroporated in suspension in the presence of lucifer yellow and incubated for 10 min. Afterward, the cells were washed by consecutive centrifugations, lysed by ultrasonication, and the fluorescence of the lysate was measured in arbitrary units on a spectrofluorometer.
Pore distribution models	**S2011 model** [31]	Electric field: 0–3.5 kV/cm [45]; 0–2 kV/cm [10] No. pulses: 1 Pulse shape: exponentially decaying [45]; rectangular pulses [10] Pulse duration: 50 μs to 21 ms [45]; 100 μs and 1 ms [10]	calcein [45] lucifer yellow [10]	electrophoresis and diffusion	Quantitative comparison with experimental measurements of calcein uptake into DU 145 prostate cancer cells exposed to exponentially decaying pulses [45] and lucifer yellow uptake into DC3F fibroblasts exposed to rectangular pulses [10].
	LL2011 model [12,30]	Electric field: 1 kV/cm [12]; 160 kV/cm [30] No. pulses: 1 Pulse shape: rectangular [12,30] Pulse duration: 6 ms [12]; 11–95 ns [30]	calcium [12] propidium [30]	electrophoresis and FASS (Field Amplified Sample Stacking)	Qualitative comparison with single-cell fluorescence microscopy of calcium uptake in CHO cells detected by Fluo3 dye [12,33] and with measurements of the percentage of Sp2 mouse myeloma cells stained with propidium [30,34].

backward rates are constants chosen based on data from different experimental reports. Addition of the MT2010 model is that the membrane can transition from P_2 further into memory state M, which represents a state of enhanced membrane perturbation and is associated with diffusive and endocytotic-like uptake. The flux of molecules $\mathbf{J_m}$ through the membrane is thus calculated as.

$$\mathbf{n}\cdot\mathbf{J_m} = \underbrace{[P_2]\ D_{X,m}\ \frac{[X]_e - [X]_i}{d_m}}_{\text{Diffusion}} + \underbrace{[M]\ D_{X,r}\ \frac{[X]_e - [X]_i}{d_m}}_{\text{Memory effect}} \tag{2}$$

where $\mathbf{n}$ is the inward vector normal to the membrane surface, $[X]_e$ and $[X]_i$ are the extra- and intracellular concentration, respectively, and d_m is the membrane thickness. P_2 state is characterized by relatively fast relaxation (characteristic time of ~1 s), whereas the M state is characterized by slow relaxation (characteristic time of several minutes). $D_{X,m}$, and $D_{X,r}$ are the diffusion coefficients for the diffusive and endocytotic-like transport, respectively. Note that MT2010 neglects electrophoretic and electroosmotic transmembrane transport.

2.2. Pore distribution models

Pore distribution models consider that pores can randomly fluctuate and change their size to minimize the membrane free energy. Pores are not described as distinct states but as a distribution function n, defined in the space of pore radius r_p such that ndr_p corresponds to the number of pores with a radius between r_p and $r_p + dr_p$. The pores can change their radius due to random thermal fluctuations and due to the act of a generalized force F_p, which corresponds to the negative gradient $F_p = -\partial W_p/\partial r_p$ of the pore energy W_p. The equation governing the dynamics of the pore distribution function is often called the Fokker-Planck equation or the Smoluchowski equation, and was first proposed for pores in planar lipid bilayers [60–62]:

$$\frac{\partial n}{\partial t} = -\frac{\partial J_p}{\partial r_p} \qquad J_p = -D_p\frac{\partial n}{\partial r_p} - \frac{D_p}{kT}n\frac{\partial W_p}{\partial r_p} \tag{3}$$

where J_p is the flux of pores in the pore radius space with D_p denoting the pore diffusion coefficient, k the Boltzmann constant, and T the temperature.

2.2.1. Models based on Krassowska and colleagues

The partial differential equation (3) is analytically unsolvable and computationally demanding when applied to describe the electroporation of whole cells. Neu and Krassowska [63] simplified equation (3) to an asymptotic ordinary differential form, which essentially describes the creation and annihilation of pores with minimum radius $r_{p,\,\min}$.

$$\frac{dN}{dt} = \underbrace{ae^{\left(\frac{U_m}{V_{ep}}\right)^2}}_{\text{Pore creation}} - \underbrace{ae^{\left(\frac{U_m}{V_{ep}}\right)^2}\frac{N}{N_0}e^{-q\left(\frac{U_m}{V_{ep}}\right)^2}}_{\text{Pore annihilation}} \tag{4}$$

where N represents the pore density (number of pores per unit area), U_m denotes the TMV, N_0 is the pore density when $U_m = 0$ V, and V_{ep}, a, and q are model parameters.

However, pores do expand in size under an electric field, as shown in molecular dynamics simulations and experiments on lipid bilayers [64–66]. Therefore, Krassowska and Filev [67] upgraded the asymptotic model by developing a numerical algorithm that tracks the expansion of individual pores, whereby each pore changes its radius according to the differential equation.

$$\frac{dr_i}{dt} = -\frac{D_p}{kT}\frac{\partial W_p}{\partial r_p} = \frac{D_p}{kT}F_p \quad j = 1, 2, \cdots, k \tag{5}$$

Note that eq. (5) is directly related to the second term in eq. (3). The algorithm of Krassowska and Filev is thus a slightly simplified version of the full equation (3). F_p denotes the force that acts to expand the pore radius and is described by eq. (6):

$$F_p = 4B\left(\frac{r_*}{r_p}\right)^4\frac{1}{r_p} - 2\pi\gamma + 2\pi\Gamma_{eff}r_p + \frac{F_{max}U_m^2}{1+\frac{r_h}{r_p+r_t}} \tag{6}$$

The first term of eq. (6) accounts for the steric repulsion between the lipid heads; the second for the force due to edge tension acting on the pore perimeter; the third for the force due to surface tension of the cell membrane; and the fourth for the electric force acting on the pore edge due to Maxwell stress. Parameter B is the steric repulsion energy, r_* is the minimum radius of hydrophilic pores, γ is the pore edge tension, Γ_{eff} is the effective surface tension of the membrane, and F_{max}, r_t, and r_h are parameters obtained as fits to numerical calculations for a toroidal pore.

Li and Lin [12] (LL2011) were the first to couple the model of Krassowska and Filev with transmembrane molecular transport. In their first paper, they simulated the uptake of calcium into single cells and its binding to the intracellular calcium indicator Fluo-3 according to the kinetic scheme.

$$Ca^{2+} + \quad Fluo \quad \underset{k_{dis}}{\overset{k_{ass}}{\rightleftarrows}} \quad CaFluo \tag{7}$$

where k_{ass} and k_{dis} are the association and dissociation rate constants, respectively. They suggested electrophoresis and diffusion as the main mechanisms of transmembrane molecular transport, which they described with Nernst-Planck equations for each considered species:

$$\begin{aligned}\frac{\partial[Ca^{2+}]}{\partial t} &= \nabla\bullet\left(D_{Ca2+}\nabla[Ca^{2+}] + \frac{z_{Ca2+}F}{RT}D_{Ca2+}[Ca^{2+}]\nabla V\right)\\ &\quad - k_{ass}[Fluo][Ca^{2+}] + k_{dis}[CaFluo]\end{aligned} \tag{8}$$

$$\begin{aligned}\frac{\partial[Fluo]}{\partial t} &= \nabla\bullet\left(D_{Fluo}\nabla[Fluo] + \frac{z_{Fluo}F}{RT}D_{Fluo}[Fluo]\nabla V\right)\\ &\quad - k_{ass}[Fluo][Ca^{2+}] + k_{dis}[CaFluo]\end{aligned}$$

$$\begin{aligned}\frac{\partial[CaFluo]}{\partial t} &= \nabla\bullet\left(D_{CaFluo}\nabla[CaFluo] + \frac{z_{CaFluo}F}{RT}D_{CaFluo}[CaFluo]\nabla V\right)\\ &\quad + k_{ass}[Fluo][Ca^{2+}] - k_{dis}[CaFluo]\end{aligned}$$

Constants D_x and z_x are the diffusion coefficient and the valence of species X. The transmembrane flux of molecules through pores is derived from the one-dimensional Nernst-Planck equation [30].

$$\mathbf{n}\bullet\mathbf{J_m} = \rho D_{m,X}\frac{u_m + \ln(\chi)}{d_m}\frac{\chi - 1}{\ln(\chi)}\frac{[X]_e - [X]_i\exp(u_m)}{(1-\chi\exp(u_m))} \tag{9}$$

where $D_{m,\,X}$ is the diffusion coefficient of species X within the pore, $\chi = \sigma_i/\sigma_e$ is the ratio between the intracellular and extracellular conductivity, and d_m is the membrane thickness. u_m is a nondimensionalized transmembrane voltage (also the Péclet number) $u_m = (z_X q_e/kT)U_m$, where q_e is the elementary charge. The scaling variable ρ is the pore area density, i.e. the local areal fraction of all pores.

LL2011 model prediction was in good agreement with qualitative measurements of calcium uptake by Gabriel and Teissie [33]. In their subsequent paper [30], they considered the intracellular uptake of fluorescent dye propidium and its binding to nucleic acids within the cytoplasm and found good agreement with the experimental measurements of Müller et al. [34]. In another subsequent paper, they combined modeling with qualitative measurements of fluorescein-dextran uptake and found good agreement as well [35].

Several other researchers have then used and/or adapted the theoretical framework layed down by Krassowska and Filev [67] and Li and Lin [12] to describe molecular transport in different systems. Mahboubi et al. [36] used the LL2011 model to study the electroporation of a cell within a microchannel. Shil et al. [37] studied the influence of cholesterol on doxorubicin uptake by modifying the term for the edge energy

in eq. (6). Goldberg et al. [38,41] included electrodeformation of the cell membrane at the whole-cell level by considering the Maxwell stress induced by the electric field. Yan et al. [43] added the effect of the Joule heating by computing the temperature increase with the heat-transfer equation and by considering the temperature dependence of the electrical properties of the aqueous solutions and the diffusion coefficients of the considered species. Guo et al. [44] included the dielectric dispersion of the membrane electrical properties. However, these subsequent models were made independently from each other, often without a thorough analysis of how the added changes affect the model prediction, and often without comparison to any experimental measurements (exceptions are the papers of Goldberg et al. [38,41]).

2.2.2. Model-based on Smith and colleagues

In parallel with Li and Lin [12], Smith et al. [31] (S2011) developed a somewhat different model of electroporation and associated molecular uptake. They also built upon the model of Krassowska and Filev [67] but modified the description of the pore creation and annihilation rate and the description of the pore energy landscape (see Suppl. Sections S4 and Table S4 for details). Furthermore, they developed a description of molecular transport through pores that consider the size, shape, and charge of the molecules and take into account the drag between the molecule and the pore wall (hindrance) and the energy cost of placing a charged solute from an aqueous environment into the membrane with low dielectric permittivity (partitioning). Hindrance and partitioning considerably reduce the electrophoretic and diffusive transport for molecules whose size is comparable to the pore size, even beyond an order of magnitude (Suppl. Fig. S4). The S2011 model was in good agreement with quantitative measurements of molecular uptake of calcein [45] and lucifer yellow [10] for a wide range of pulse durations (from 50 μs to 20 ms). The model was subsequently used by Son et al. [46,47] to study the uptake of propidium, calcein, and calcium following pulses of different duration and number. The S2011 model was later adapted by Mi et al. [48,49]. In their first paper [48], they derived a simplified expression for membrane surface tension from the Maxwell stress tensor to account for mechanical stress caused by electrodeformation. They also made slight modifications to the expression for the steric pore energy, the pore destruction rate, and the value of the maximum pore radius, which they have not discussed. In their second paper [49], they divided the pores into three classes based on their radius: unstable reversible pores with a radius < 5 nm, stable reversible pores with a radius between 5 nm and r_d, and irreversible pores with a radius larger than r_d, where $r_d \approx 20$ nm corresponds to the global maximum in the pore energy landscape. Although their pore classification is not fully consistent with the original theoretical description of the pore population [31,60,68], they showed that their modifications improve the agreement with their experimental measurements.

2.3. Other phenomenological models

The last group of models in Table 1 are models that have a strong phenomenological component, especially with respect to how the increase in membrane permeability due to electroporation is described. Puc et al. [10] developed a two-compartment pharmacokinetic model, representing the extracellular and intracellular space, and described the transmembrane transport of fluorescent dye lucifer yellow with a phenomenological function which parameters were fitted to their experimental measurements. Pavlin et al. [50 51] designed experiments that enabled them to estimate the fraction of pores formed in the membrane. Their theoretical analysis pointed to two distinct types of pores, short-lived pores that are numerous but exist mainly during the presence of an electric field, and long-lived pores that are smaller in number but persist for seconds to minutes after the pulse exposure and accumulate when applying multiple pulses. Their model uses a phenomenological description of how the fraction of pores depends on the amplitude and number of applied pulses, and the model was not developed to the extent that would enable spatiotemporal simulations of single-cell electroporation. Unlike most other groups, Leguebe et al. [52] developed a model which attributes the increase in membrane permeability not only to lipid pores but also to lipid peroxidation. The pores are considered short-lived whereas the increase in permeability due to lipid peroxidation is considered long-lived. The mathematical description for pores has a mechanistic background and is derived in a (strongly) simplified form from eq. (4). However, the increase in membrane permeability due to lipid peroxidation, and how it relates to lipid pores, is described in a phenomenological way with a simple mathematical function without any mechanistic background. The multiscale model of Dermol-Černe et al. [42] connects a mathematical description of molecular transport at the single-cell level and the tissue level; however, the increase in membrane permeability was determined experimentally and was not related to any mechanistic description of membrane electroporation. Finally, Sweeney et al. [56] developed a two-stage ordinary differential equation model to describe electroporation and molecular transport, which yielded good agreement with quantitative measurements of propidium iodide uptake. Nevertheless, the model is based on two-stage ordinary differential equations of phenomenological origin, whereby all model parameters need to be obtained based on fits to experimental measurements.

Since all phenomenological models largely depend on the subset of experimental measurements for which they were fitted, we have excluded them from further testing in our study.

3. Results and Discussion

The main aim of our study was to critically examine whether any of the existing single-cell electroporation models is universal enough to describe electroporation and the associated molecular transport generally for all different pulse parameters used in electroporation applications related to animal cells. We approached our question by first surveying the literature. We searched for mechanistic mathematical models designed to describe the phenomenon of electroporation and induced transmembrane transport of small molecules at the single-cell level with full spatiotemporal resolution. We selected three representative models, which met all our selection criteria: MT2010 [29], S2011 [31], and LL2011 [12] models. We then tested these models against experimental measurements of intracellular uptake of different small molecules made by Puc et al. [10]., Canatella et al. [45], Sozer et al. [69], and Gabriel and Teissie [33].

Showing how each selected model describes all selected experiments would be lengthy and unnecessary to reach the main conclusions of the study. Instead, we show different examples that illustrate the shortcomings of current electroporation models and provide guidelines for further development of these models. In this light, the Results and Discussion are divided into four sections, according to the four main takeaway messages we would like to convey:

1. Qualitative validation is not sufficient to establish the goodness/validity of a model;
2. Quantitative validation in a fixed time point does not necessarily indicate the correct description of the kinetics of the uptake;
3. Certain experiments are not selective enough for model validation;
4. Further development of mechanistic models requires a better understanding of the molecular mechanisms of electroporation.

3.1. Qualitative validation is not sufficient to establish the goodness/validity of a model

The MT2010 [29] model was originally compared with results from Kotnik et al. [32], who reported measurements of intracellular uptake of lucifer yellow induced by 1-ms-long pulses of different shapes. The model correctly predicted the greatest uptake for a rectangular pulse,

followed by pulses with sinusoidal and triangular shapes. The model further correctly predicted a decrease in transport when modulating rectangular pulses with a 50 kHz sinewave. Finally, the model correctly predicted no change in transport when applying a unipolar or bipolar rectangular pulse and when changing the rise time of a unipolar rectangular pulse from 2 μs to 100 μs. However, the comparison was only qualitative, as the reported lucifer yellow measurements were in arbitrary fluorescence units. Therefore, we tested if the MT2010 model can quantitively simulate the experimental study of Puc et al. [10] in which the intracellular concentration of lucifer yellow was quantified 10 min after exposing cells to a single 100 μs or 1 ms rectangular pulse of different amplitudes [10]. Fig. 2 shows that the uptake of lucifer yellow increases with increasing applied electric field both in the model and in the experiment. However, the MT2010 model overestimates the experimental values of intracellular concentration by almost an order of magnitude. For both pulse durations, the model fails to quantitatively reproduce the experimental data. This demonstrates how qualitative comparison between model and experiment is not sufficient for model validation.

3.2. *Quantitative validation in a fixed time point does not necessarily indicate the correct description of the kinetics of the uptake*

The S2011 model was originally compared with quantitative experimental measurements of lucifer yellow uptake from Puc et al. [10] and calcein uptake from Canatella et al. [45] showing excellent agreement (Fig. 3 shows our reproduction of the modeling results presented in [31]). This agreement is impressive, as there are many differences in the experiments of Canatella et al. and Puc et al. Namely, Canatella et al. measured the uptake of calcein in DU 145 prostate cancer cells exposed to exponentially decaying pulses, whereas Puc et al. measured the uptake of lucifer yellow in DC-3F spontaneously transformed fibroblasts exposed to rectangular pulses. Furthermore, the duration of the electric pulses used in these experiments collectively spans nearly 3 orders of magnitude (50 μs to 21 ms). However, we need to consider that the agreement between the model and experiments was obtained after fitting the values of five model parameters, including the pore diffusion coefficient D_p, symmetric pore creation rate β, asymmetric pore creation rate α, maximum pore radius $r_{p,\max}$, and characteristic time of pore closure τ_p. When fitting many parameters of a complex model to a given dataset, two main problems can occur. The first problem is that such a complex model can be too flexible and can be fitted to almost any data, which prevents one from critically assessing the validity of the model. The second problem is that multiple combinations of parameter values can yield an adequate fit to the given dataset. Therefore, it is crucial to measure or assess independently as many model parameters as possible. While the first four listed parameters (D_p, β, α, $r_{p,\max}$) cannot (yet) be directly measured experimentally, membrane resealing time can be.

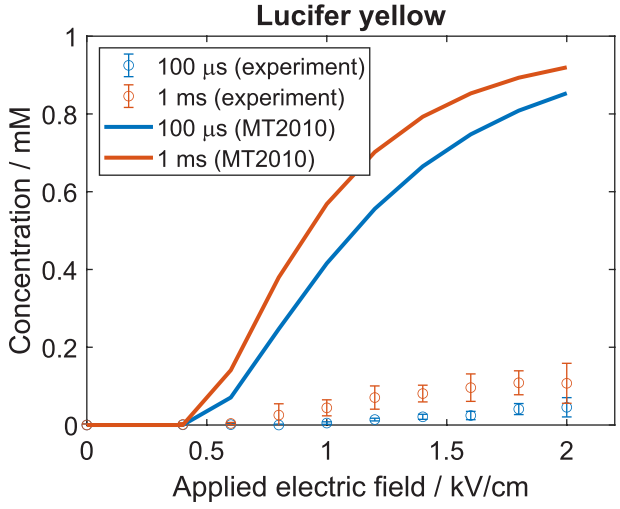

Fig. 2. Intracellular concentration of lucifer yellow as a function of the applied electric field strength upon exposure to a single 100 μs or 1 ms pulse. Circles and solid lines, respectively, show the experimental measurements of intracellular concentration from Puc et al. [10] and the results of the MT2010 model.

Recently, Sözer et al. [69] reported the first spatially resolved quantitative measurements of the kinetics of intracellular uptake of calcein, propidium, and yo-pro1 during and after exposure of U937 histiocytic lymphoma cells to either a single 220 μs, 2.5 kV/cm pulse or ten 6 ns, 200 kV/cm pulses. The results of Sözer et al. thus offer an excellent opportunity to further test the validity of the S2011 model. Calcein is fluorescent by itself, whereas the fluorescence of propidium and yo-pro1 increases dramatically upon binding to nucleic acids in the cytoplasm. Consequently, for propidium and yo-pro1 we need to take into account the binding reaction with nucleic acids, as the detected fluorescent signal is emitted practically exclusively from the bound molecules. Out of the three molecules considered, we chose to focus on calcein and propidium; calcein, because the model has already been used to model calcein uptake in the experiments of Canatella et al. [45], and propidium, because the binding reaction between propidium and nucleic acids in the cytoplasm has already been described and modeled in previous studies [30,70–72].

To compare the S2011 model with experiments of Sözer et al. we adapted the values for the cell radius and extracellular medium conductivity to correspond to U937 cells and RPMI growth medium, respectively, and we also considered the shape of the pulse waveforms used by Sözer et al. (Suppl. Fig. S15). Measurements of Sözer et al. upon exposing the cells to a 220 μs pulse, specifically the kinetics of calcein uptake, showed that membrane resealing took tens of seconds (Fig. 4a). Fitting the data to a first-order exponential function gave a resealing time constant of 25 s (Suppl. Fig. S14). Thus, we also changed the value of τ_p in the S2011 model from 4 s to 25 s. Other parameter values were kept the same as for Puc et al. and Canatella et al. experiments (see Suppl. Tables S4, S5, and S6 for details).

We first computed the molecular uptake induced by 220 μs, 2.5 kV/cm pulse. Interestingly, the total uptake of calcein predicted by the S2011 model was in good agreement with the experiment. However, the model failed to reproduce the uptake kinetics of both calcein and propidium. Fig. 4b shows that, for both molecules, the electrophoretic uptake during the pulse is dramatically overestimated, as can be seen from the rapid jump in the intracellular concentration around time $t = 5$ s when the pulse is applied. Such a jump is not observed in the experimental measurements (Fig. 4a). Furthermore, the measurements of the propidium uptake showed that the uptake is greater on the cathodic (- electrode) compared to the anodic (+ electrode) cell side, not *vice versa* as suggested by the model. Since propidium is positively charged (valence $z_{Pr} = +2$), greater uptake on the cathodic side can only be explained if diffusion is the dominant mechanism of molecular transport and if the cathodic side becomes more permeable compared to the anodic side. The latter is indeed assumed based on experimental observations in the original S2011 model. Therefore, we made additional calculations, where we neglected the electrophoretic transport: we considered that molecules can move only due to concentration gradient but not due to the electric field. The resulting concentration profiles were more reasonable but quantitatively more than an order of magnitude too low (Suppl. Fig. S17). Note that in the S2011 model all pores shrink to a minimum size after the pulse, whereby the smaller the minimum pore size, the more the molecular transport through pores is hindered. Therefore, we additionally increased the minimum pore radius from 1.0 nm to 1.35 nm to allow greater molecular flux, and the model came in reasonable agreement with the experimental measurement (Fig. 4c). The model could describe the symmetric uptake of calcein and the asymmetric uptake of propidium with the dominant transport occurring on the cathodic side. This exercise demonstrates

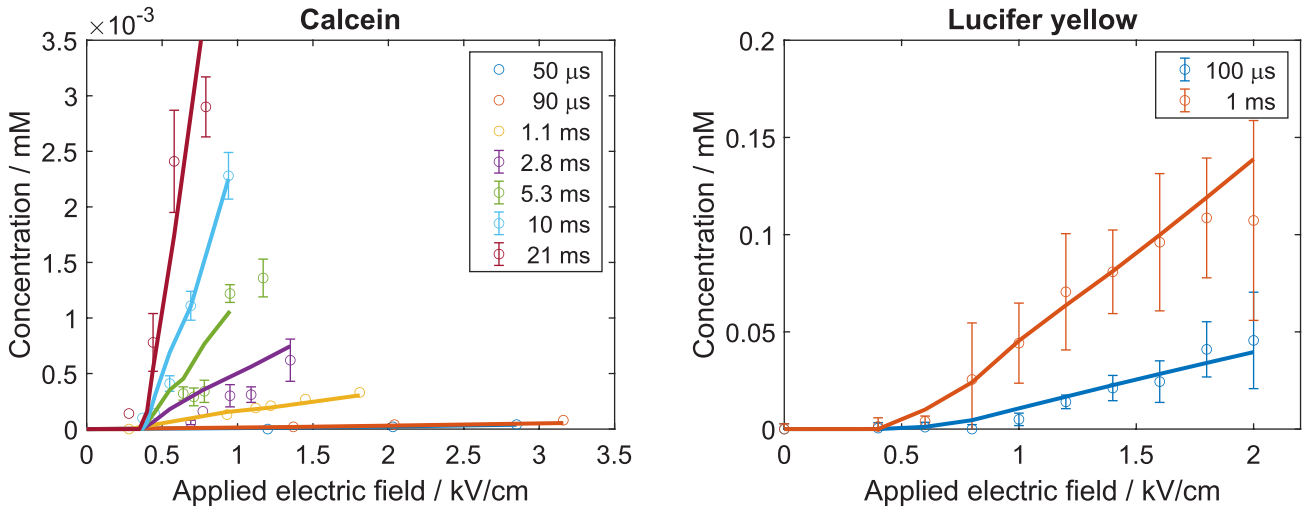

Fig. 3. Final intracellular concentration of calcein and lucifer yellow internalized after exposing cells to a single pulse of a given duration and a given amplitude. Circles denote experimental measurements carried out by Canatella et al. [45] and Puc et al. [10] for calcein and lucifer yellow, respectively. Solid lines show the prediction of the S2011 model.

how a complex model such as S2011 can rather quickly be adapted to a given experiment; by making a few well-thought, yet arbitrary changes to the model, we were able to bring the model in good agreement with the experimental measurements.

We next computed the uptake of calcein and propidium upon exposure to ten 6 ns, 200 kV/cm pulses, which was also measured by Sözer et al [69]. We again consider the original S2011 model with electrophoretic and diffusive transport and with a minimum pore radius of 1.0 nm. Pulses with a duration of 6 ns are extremely short, therefore electrophoretic uptake is practically negligible and most of the transport occurs after the pulses, as can be seen, both in the experiment and the model (Fig. 5). However, the model disagrees quantitatively with the experiment. The comparison between Fig. 5a and Fig. 5b shows that the computed change in the normalized concentration of calcein and propidium is, respectively, about 3x and 10x higher than the measured one. Furthermore, the measurements show asymmetric uptake of propidium, with greater uptake on the anodic side, whereas the model predicts symmetric uptake of propidium from the anodic and cathodic sides. Another discrepancy between the model and experiment is that the model predicts almost equal molecular uptake induced by a single 6 ns pulse as induced by ten 6 ns pulses (Fig. 5b). While Sözer et al. have not reported the uptake of calcein and propidium upon a single 6 ns pulse, they have shown that the uptake of yo-pro-1 induced by a single 6 ns pulse is about an order of magnitude lower than induced by ten 6 ns pulses [69]. The fact that the S2011 model predicts similar uptake for single and multiple pulses has also been shown by Son et al. [47].

Overall, the results presented in this section demonstrate that quantitative measurements of the kinetics of molecular uptake are crucial to assess whether the model correctly describes the dominant transport mechanisms (electrophoresis, diffusion, etc.). Quantitative measurements of the total molecular uptake at a fixed point in time are not sufficient for this purpose. Furthermore, the results show how the characterization of the asymmetry of molecular transport at the cathodic and anodic side of the cell provides important information about the mechanism of transmembrane molecular transport and should be included when validating an electroporation model. Finally, the results indicate that to develop and validate a mechanistic electroporation model, the model should be tested against experiments using single and multiple pulses, as well as a wide range of pulse durations, including nanosecond pulses.

3.3. Certain experiments are not selective enough for model validation

The LL2011 model [12] was originally compared to the experimental measurements of calcium uptake into Chinese hamster ovary (CHO) cells measured by Gabriel and Teissié [33] and showed good agreement. We performed similar calculations and compared the predictions of the LL2011 and S2011 models. Note that the S2011 model is related to the LL2011 model with respect to the description of pore dynamics, but differs in the values of the model parameters and the description of the transmembrane molar flux (see Section 2.2.2 and Suppl. Section S4). Despite their differences, both models predict practically identical concentration profiles, in good agreement with the experiment (Fig. 6). However, when we use the LL2011 model to calculate, e.g., the uptake of lucifer yellow measured by Puc et al. [10], the model overestimates the final intracellular concentration by an order of magnitude (Fig. 6d). This exercise shows how models, which appear valid for a specific experiment, can fail in a broader context when applied to a different experiment. It further shows that the experiment of Gabriel and Teissié is not in itself suitable for validating an electroporation model, as both S2011 and LL2011 models can describe the experimental results well despite their differences in describing poration dynamics and molecular transport. Thus, experiments intended for validating an electroporation model need to be carefully and critically designed.

3.4. Further development of mechanistic models requires a better understanding of the molecular mechanisms of electroporation

All models tested in our study reached limitations when quantitatively confronted with different experimental measurements covering a wide range of pulse parameters. Thus, the models need to be used with care when being applied outside the range of parameters, for which they have been developed, and necessarily combined with experimental validation. While no mathematical model can be truly universal in any field of study, the tested models (and variations thereof) have often been used as though they can be commonly applied for any electroporation experiment (see Table 2 reporting the range of pulse parameters, cell lines, and molecules considered with the tested models, as well as the studies listed in Table 1 and the references therein). Our study shows that there is a need for further development of mechanistic electroporation models to assess the associated molecular transport for the entire range of experimental conditions used in electroporation applications. One strategy would be to further optimize the values of the existing model's parameters and/or replace certain expressions/equations,

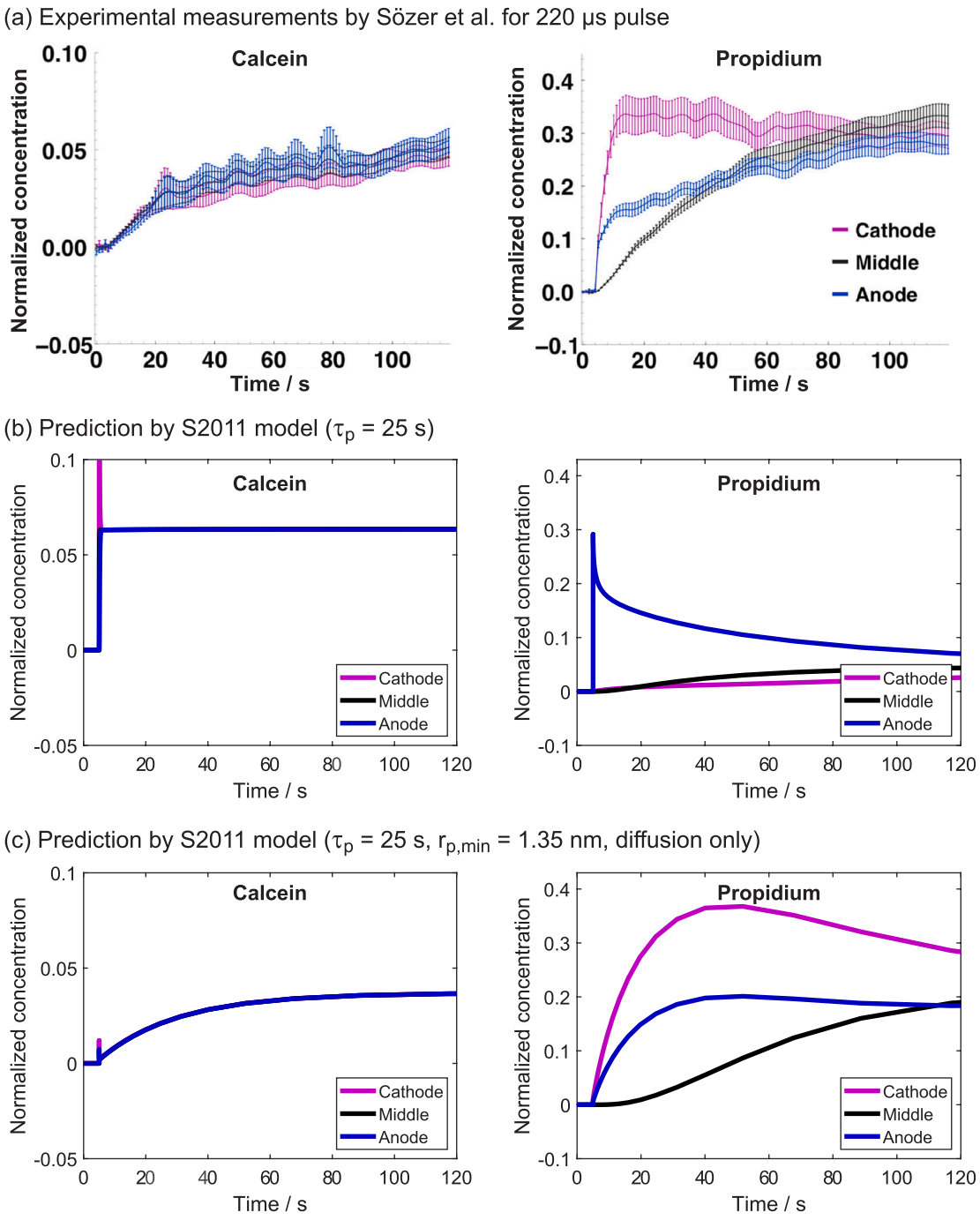

Fig. 4. Intracellular concentration of calcein and propidium upon exposure to a single 220 µs, 2.5 kV/cm pulse. The intracellular concentration is normalized to the initial extracellular concentration. For propidium, the concentration of bound molecules, normalized to the initial concentration of extracellular free propidium, is shown. (a) Experimental measurements, reproduced with permission from Sözer et al. [69]. (b) Modeling results using default model parameters (Suppl. Table S4). (c) Modeling results when neglecting electrophoretic transport and increasing the minimum pore radius to 1.35 nm.

which have been oversimplified in a model, with their unsimplified version. However, this strategy leads to a dead-end, if a model is in its essence based on incorrect assumptions.

Almost all current electroporation models assume that the increase in cell membrane permeability can be attributed to a single mechanism: the creation of pores in the lipid domains of the cell membrane, which passively close upon removal of the external electric field. In addition, most models assume that all pores exhibit similar kinetic behavior. However, accumulating evidence from experiments and simulations on model systems speaks against these assumptions. Firstly, if lipid pores formed by an electric field are the sole mechanism of increased membrane permeability, such pores need to stay open for minutes after exposure to the electric field to corroborate the experimentally measured slow uptake/leakage of ions and molecules. Such a long pore closure time requires one to assume that there exists a large energy barrier of several 10 *kT* for pore closure [31,73]. This assumption does not agree with free energy calculations for pores in pure lipid bilayers [74] as well as with experimental measurements on pure lipid systems [75,76]. Secondly, electroporation has been associated with oxidative damage of polyunsaturated lipids through experiments on pure lipids vesicles and cells *in vitro* [77,78]. Oxidative damage can lead to partial cleavage of the lipids tails (i.e., leads to secondary peroxidation

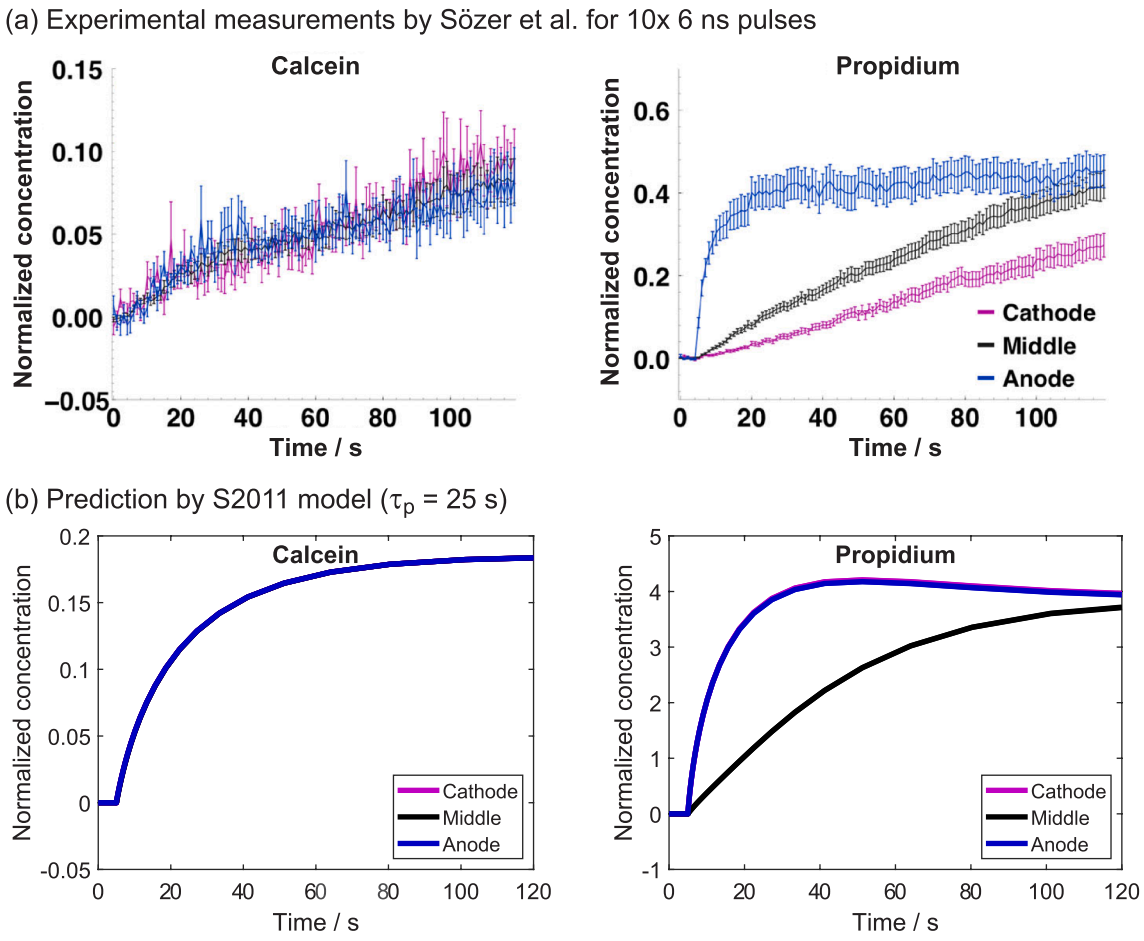

Fig. 5. Intracellular concentration of calcein and propidium upon exposure to 6 ns, 200 kV/cm pulses. The intracellular concentration is normalized to the initial extracellular concentration. (a) Experimental measurements were reproduced with permission from Sözer et al. [69]. (b) Modeling results using default S2011 model parameters. Note the different y-axes in (a) and (b). Note also that the normalized propidium concentration exceeds 1, which is possible because most propidium molecules bind to nucleic acids, allowing a continuous flow of free propidium into the cell (until all binding sites on nucleic acids are occupied).

products), whereby in such oxidatively damaged membrane lesions, pore-like defects can spontaneously form even in the absence of an electric field [79,80]. Such pore-like defects are different from the "conventional" lipid pores that form directly by an electric field: the kinetics of their formation is different, they do not need an electric field to stay open, and they can disappear only after lateral diffusion of oxidized lipids or by cell membrane repair mechanisms. Therefore, such pores are more likely to explain the persistent increase in cell membrane permeability following exposure to electric pulses. Thirdly, computational simulations supported by electrophysiological measurements suggest that pores can nucleate within some membrane proteins, specifically voltage-gated ion channels, causing protein denaturation [81,82]. Such complex pores, stabilized by both lipids and protein residues, can be more stable than pure lipid pores and, to disappear, the damaged proteins need to be replaced by the cell repair mechanisms. Therefore, protein denaturation is also a possible mechanism of persistent increase in cell membrane permeability due to electric pulses. Finally, experiments have shown that pore formation and/or expansion is affected by the actin cytoskeleton, either via actin's influence on lipid organization or the mechanical properties of the membrane [83,84]. At the same time, the actin cytoskeleton can become disrupted by electroporation [85]. This points to a complex role of the actin cytoskeleton in the increased membrane permeability.

Identification of the different possible mechanisms of increased membrane permeability prompts us to understand electroporation in the sense of multiple types of pores/defects that can form simultaneously in the cell membrane, but by different molecular mechanisms. This view is related to the distinction between short-lived and long-lived pores, proposed earlier by Pavlin et al. [50]. Interestingly, Schmeer et al. [24], who contributed to the development of pore states models, noted in the paper that their model would be in agreement with experiments even if they considered that P_1 and P_2 pore states form independently and in parallel, rather than in series. Phenomenological models are also suggesting distinct types of increased membrane permeability with different relaxation times, as discussed in Section 2.3. Overall, there is ample evidence in the literature, supporting the view of multiple distinct types of pores/defects occurring in electroporation. However, the main challenge of adding these different types of pores/defects to an electroporation model is the lack of knowledge required for developing mathematical expressions governing the formation kinetics and dynamic behavior of these pores. Filling the gaps in knowledge will require multiscale approaches including molecular modeling such as molecular dynamics simulations together with enhanced sampling methods to determine the free energy barriers for the formation of the different types of pores. In addition, experiments on model membrane systems of increasing complexity, including lipid bilayers with complex lipid mixtures, bilayers containing membrane proteins and/or cytoskeletal components, as well as cells genetically engineered to express selected cellular components (or knock out the expression) can be designed to provide the required information [82–84,86,87]. Further studies on the

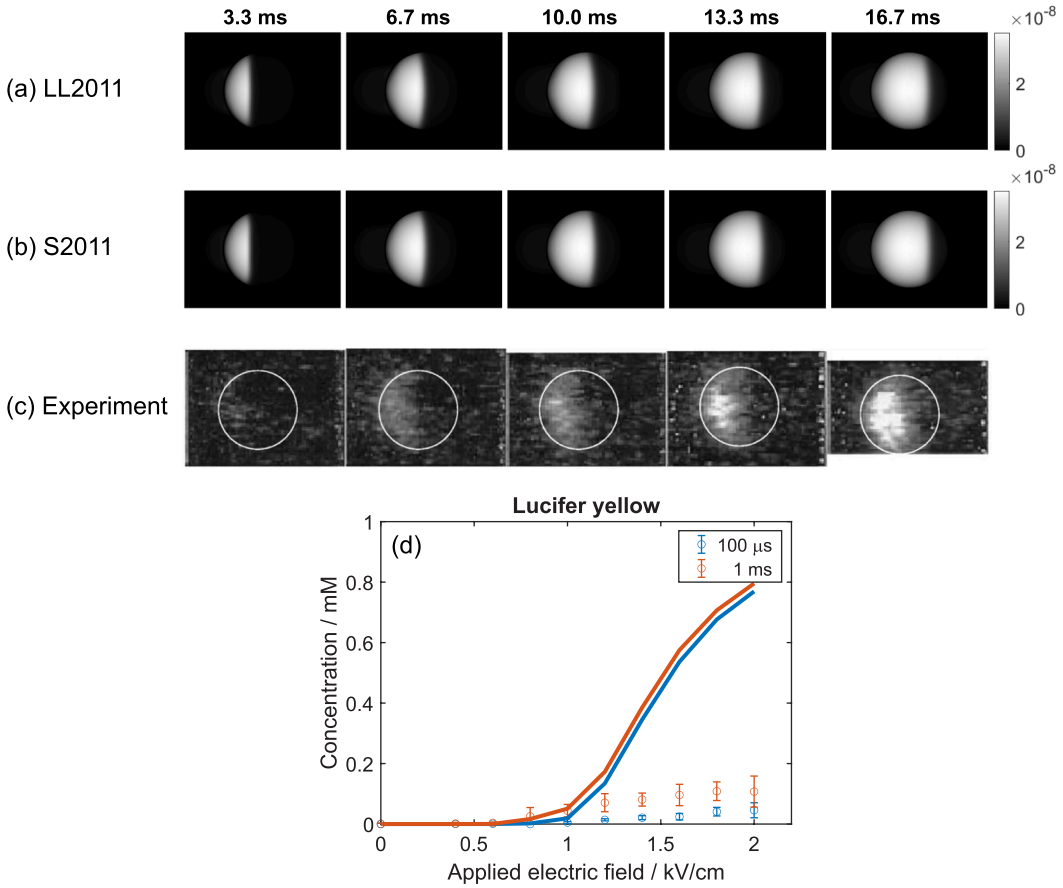

Fig. 6. Comparison between S2011 and LL2011 model. (a,b) Calculations of the intracellular concentration of calcium bound to Fluo-3 at different times after the onset of a 6 ms pulse. The intracellular concentration is presented as would appear on an epifluorescence microscope. (c) Corresponding experimental results, reproduced with permission from Gabriel and Teissié [33]. (d) Intracellular uptake of lucifer yellow, as measured by Puc et al. [10] (circles with error bars) and as predicted by the LL2011 model (solid lines). The model overestimates the intracellular uptake by roughly an order of magnitude.

biological mechanisms which could help cells repair the membrane after electroporation are also needed [88]. Much inspiration on how to develop the required mathematical expressions can actually be found in the historical development leading to the existing models of electroporation and molecular transport [24,25,31,68].

4. Conclusions and recommendations

Our study concludes that none of the existing single-cell models describing electroporation and the associated transmembrane molecular transport is universal enough to describe the entire range of experimental measurements of small molecule transport through the membrane. While upgrading and/or adapting the existing models might enable some progress, we anticipate that investments into a better understanding of the molecular mechanisms of the increased membrane permeability are more likely to result in successful development of a mechanistic electroporation model that can be applied for the entire range of pulse parameters used in electroporation applications (is such a model can exist). To this end, insights from molecular modeling and experiments on different model membrane systems with increasing complexity will undoubtedly play one of the crucial roles. Another crucial role will be played by well-designed and well-reported experimental measurements against which an electroporation model can be compared and validated [89]. Based on our findings we suggest that the experiments designed to validate electroporation models include:

- quantitative measurements of molecular uptake (or leakage);
- time courses of the intracellular concentration(s);
- 2D profiles of the intracellular concentration (to show asymmetric or symmetric uptake);
- measurements carried out over a wide range of pulse durations and amplitudes and also considering different number of pulses;
- measurements carried out for different molecules (at least one anionic and one cationic to determine the role of electrophoresis in the total uptake).

The experiments further need to report on cell size and shape, cell density, the conductivity of the extracellular electroporation medium, pulse shape, exact values of molecules characteristics (concentration and, if possible, the diffusion constant within the extracellular/intracellular medium), and temperature at which the experiments were performed, as these are all parameters which affect the modeling results but are in practice often not all reported. The experiments should also estimate the electric field strength experienced by the cells correcting for chemical oxidation or electrolytic reaction that might reduce the voltage established on the sample. For microscopic images, relevant details of the imaging configuration should be reported, for example, the focal depth in wide-field microscopy or the thickness of the focal plane in confocal microscopy.

Finally, we encourage authors to share their models through open access repositories, as we often find that the descriptions of the models in the publications do not provide sufficient detail and/or contain typographic errors that impede reproducibility and reuse of the reported models.

Declaration of Competing Interest

The authors declare that they have no known competing financial interests or personal relationships that could have appeared to influence the work reported in this paper.

Data availability

All models used in this study are available at https://github.com/learems/EPmodels-Electroporation-MolTransport.

Acknowledgements

The study was supported by the Slovenian Research Agency (ARRS) within project no. J2-2503. LR gratefully acknowledges funding from the Europen Comission via European Union's Horizon 2020 research and innovation program under the Marie Skłodowska-Curie grant agreement No. 893077. PEB gratefully acknowledges funding from the ENW-M-2 project (project number OCENW.M20.308, ROCKET) which is financed by the Dutch Research Council (NWO). The authors thank Damijan Miklavčič for his useful comments to the manuscript, and Pim Reijnierse for assistance with some of the preliminary numerical calculations.

Appendix A. Supplementary material

Supplementary data to this article can be found online at https://doi.org/10.1016/j.bioelechem.2022.108216.

References

[1] J. Yang, Y. Huang, X.-B. Wang, F.F. Becker, P.R. Gascoyne, Cell separation on microfabricated electrodes using dielectrophoretic/gravitational field-flow fractionation, Anal. Chem. 71 (5) (1999) 911–918.
[2] D. Issadore, T. Franke, K.A. Brown, R.M. Westervelt, A microfluidic microprocessor: controlling biomimetic containers and cells using hybrid integrated circuit/microfluidic chips, Lab Chip 10 (21) (2010) 2937–2943.
[3] B. Geboers, et al., High-voltage electrical pulses in oncology: irreversible electroporation, electrochemotherapy, gene electrotransfer, electrofusion, and electroimmunotherapy, Radiology 295 (2) (2020) 254–272.
[4] L. Lambricht, A. Lopes, S. Kos, G. Sersa, V. Préat, G. Vandermeulen, Clinical potential of electroporation for gene therapy and DNA vaccine delivery, Expert opinion on drug delivery 13 (2) (2016) 295–310.
[5] K. R. Foster and H. P. Schwan, "Dielectric properties of tissues," *CRC handbook of biological effects of electromagnetic fields*, pp. 27–96, 1986.
[6] T. Kotnik, L. Rems, M. Tarek, D. Miklavčič, Membrane electroporation and electropermeabilization: mechanisms and models, Annu. Rev. Biophys. 48 (2019) 63–91.
[7] T. Kotnik, F. Bobanović, D. Miklavčič, Sensitivity of transmembrane voltage induced by applied electric fields—a theoretical analysis, Bioelectrochem. Bioenerg. 43 (2) (1997) 285–291.
[8] C. Rosazza, S. Haberl Meglic, A. Zumbusch, M.-P. Rols, D. Miklavcic, Gene electrotransfer: a mechanistic perspective, Curr. Gene Ther. 16 (2) (2016) 98–129.
[9] D.S. Dimitrov, A.E. Sowers, Membrane electroporaton—fast molecular exchange by electroosmosis, Biochimica et Biophysica Acta (BBA)-Biomembranes 1022 (3) (1990) 381–392.
[10] M. Puc, T. Kotnik, L.M. Mir, D. Miklavčič, Quantitative model of small molecules uptake after in vitro cell electropermeabilization, Bioelectrochemistry 60 (1–2) (2003) 1–10.
[11] M.M. Sadik, J. Li, J.W. Shan, D.I. Shreiber, H. Lin, Quantification of propidium iodide delivery using millisecond electric pulses: experiments, Biochimica et Biophysica Acta (BBA)-Biomembranes 1828 (4) (2013) 1322–1328.
[12] J. Li, H. Lin, Numerical simulation of molecular uptake via electroporation, Bioelectrochemistry 82 (1) (2011) 10–21.
[13] G. Pucihar, T. Kotnik, D. Miklavčič, J. Teissié, Kinetics of transmembrane transport of small molecules into electropermeabilized cells, Biophys. J . 95 (6) (2008) 2837–2848.
[14] E.B. Sözer, C.F. Pocetti, P.T. Vernier, Transport of charged small molecules after electropermeabilization—drift and diffusion, BMC biophysics 11 (1) (2018) 1–11.
[15] J.-M. Escoffre, T. Portet, L. Wasungu, J. Teissié, D. Dean, M.-P. Rols, What is (still not) known of the mechanism by which electroporation mediates gene transfer and expression in cells and tissues, Mol. Biotechnol. 41 (3) (2009) 286–295.
[16] T. Kotnik, W. Frey, M. Sack, S.H. Meglič, M. Peterka, D. Miklavčič, Electroporation-based applications in biotechnology, Trends Biotechnol. 33 (8) (2015) 480–488.
[17] S. Mahnič-Kalamiza, E. Vorobiev, D. Miklavčič, Electroporation in food processing and biorefinery, The Journal of membrane biology 247 (12) (2014) 1279–1304.
[18] D.Y. Lyon, J. Pivetal, L. Blanchard, T.M. Vogel, Bioremediation via in situ electrotransformation, Biorem. J. 14 (2) (2010) 109–119.
[19] Z. Chen, W.G. Lee, Electroporation for microalgal biofuels: a review, Sustainable Energy Fuels 3 (11) (2019) 2954–2967.
[20] C.B. Arena, et al., High-frequency irreversible electroporation (H-FIRE) for non-thermal ablation without muscle contraction, Biomed. Eng. Online 10 (1) (2011) 1–21.
[21] K. Čepurnienė, P. Ruzgys, R. Treinys, I. Šatkauskienė, S. Šatkauskas, Influence of plasmid concentration on DNA electrotransfer in vitro using high-voltage and low-voltage pulses, The Journal of Membrane Biology 236 (1) (2010) 81–85.
[22] M.-P. Rols, J. Teissié, Electropermeabilization of mammalian cells to macromolecules: control by pulse duration, Biophys. J . 75 (3) (1998) 1415–1423.
[23] J.C. Weaver, K.C. Smith, A.T. Esser, R.S. Son, T.R. Gowrishankar, A brief overview of electroporation pulse strength–duration space: A region where additional intracellular effects are expected, Bioelectrochemistry 87 (2012) 236–243.
[24] M. Schmeer, T. Seipp, U. Pliquett, S. Kakorin, E. Neumann, Mechanism for the conductivity changes caused by membrane electroporation of CHO cell-pellets, PCCP 6 (24) (2004) 5564–5574.
[25] E. Neumann, K. Tönsing, S. Kakorin, P. Budde, J. Frey, Mechanism of electroporative dye uptake by mouse B cells, Biophys. J . 74 (1) (1998) 98–108.
[26] K.A. DeBruin, W. Krassowska, Modeling electroporation in a single cell. I. Effects of field strength and rest potential, Biophys. J . 77 (3) (1999) 1213–1224.
[27] M. Hibino, H. Itoh, K. Kinosita Jr, Time courses of cell electroporation as revealed by submicrosecond imaging of transmembrane potential, Biophys. J . 64 (6) (1993) 1789–1800.
[28] S. Sachdev, T. Potočnik, L. Rems, D. Miklavčič, Revisiting the role of pulsed electric fields in overcoming the barriers to in vivo gene electrotransfer, Bioelectrochemistry (2021), 107994.
[29] D. Miklavcic, L. Towhidi, Numerical study of the electroporation pulse shape effect on molecular uptake of biological cells, Radiology and oncology 44 (1) (2010) 34–41.
[30] J. Li, W. Tan, M. Yu, H. Lin, The effect of extracellular conductivity on electroporation-mediated molecular delivery, Biochimica et Biophysica Acta (BBA)-Biomembranes 1828 (2) (2013) 461–470.
[31] K.C. Smith, A unified model of electroporation and molecular transport, PhD Thesis, Massachusetts Institute of Technology (2011).
[32] T. Kotnik, G. Pucihar, M. Reberšek, D. Miklavčič, L.M. Mir, Role of pulse shape in cell membrane electropermeabilization, Biochimica et Biophysica Acta (BBA)-Biomembranes 1614 (2) (2003) 193–200.
[33] B. Gabriel, J. Teissie, Time courses of mammalian cell electropermeabilization observed by millisecond imaging of membrane property changes during the pulse, Biophys. J . 76 (4) (1999) 2158–2165.
[34] K.J. Müller, V.L. Sukhorukov, U. Zimmermann, Reversible electropermeabilization of mammalian cells by high-intensity, ultra-short pulses of submicrosecond duration, The Journal of membrane biology 184 (2) (2001) 161–170.
[35] M.M. Sadik, et al., Scaling relationship and optimization of double-pulse electroporation, Biophys. J . 106 (4) (2014) 801–812.
[36] M. Mahboubi, S. Movahed, R. Abardeh, V. Hoshyargar, Theoretical Study of Molecular Transport Through a Permeabilized Cell Membrane in a Microchannel, J. Membr. Biol. 250 (3) (Jun. 2017) 285–299, https://doi.org/10.1007/s00232-017-9961-2.
[37] P. Shil, K. B. Achary, and K. Alagarasu, "Numerical analyses of electroporation-mediated doxorubicin uptake in eukaryotic cells: role of membrane cholesterol content," 2018.
[38] E. Goldberg, C. Suárez, M. Alfonso, J. Marchese, A. Soba, G. Marshall, Cell membrane electroporation modeling: A multiphysics approach, Bioelectrochemistry 124 (2018) 28–39.
[39] H. Engelhardt, E. Sackmann, On the measurement of shear elastic moduli and viscosities of erythrocyte plasma membranes by transient deformation in high frequency electric fields, Biophys. J . 54 (3) (1988) 495–508.
[40] C. Mauroy, I. Rico-Lattes, J. Teissié, M.-P. Rols, Electric destabilization of supramolecular lipid vesicles subjected to fast electric pulses, Langmuir 31 (44) (2015) 12215–12222.
[41] E. Goldberg, A. Soba, D. Gandía, M.L. Fernández, C. Suárez, Coupled mathematical modeling of cisplatin electroporation, Bioelectrochemistry 140 (2021), 107788.
[42] J. Dermol-Černe, J. Vidmar, J. Ščančar, K. Uršič, G. Serša, D. Miklavčič, Connecting the in vitro and in vivo experiments in electrochemotherapy-a feasibility study modeling cisplatin transport in mouse melanoma using the dual-porosity model, J. Control. Release 286 (2018) 33–45.
[43] Z. Yan, C. Hao, L. Yin, K. Liu, J. Qiu, Simulation of the Influence of Temperature on the Dynamic Process of Electroporation Based on Finite Element Analysis, IEEE Trans. Plasma Sci. 49 (9) (2021) 2839–2850.
[44] F. Guo, K. Qian, L. Zhang, X. Liu, H. Peng, Multiphysics modelling of electroporation under uni-or bipolar nanosecond pulse sequences, Bioelectrochemistry 141 (2021), 107878.
[45] P.J. Canatella, J.F. Karr, J.A. Petros, M.R. Prausnitz, Quantitative study of electroporation-mediated molecular uptake and cell viability, Biophys. J . 80 (2) (2001) 755–764.
[46] R.S. Son, K.C. Smith, T.R. Gowrishankar, P. Thomas Vernier, P. Thomas Vernier, J. C. Weaver, Basic Features of a Cell Electroporation Model: Illustrative Behavior for Two Very Different Pulses, The Journal of Membrane Biology (2014), https://doi.org/10.1007/s00232-014-9699-z.
[47] R.S. Son, T.R. Gowrishankar, K.C. Smith, J.C. Weaver, Modeling a conventional electroporation pulse train: decreased pore number, cumulative calcium transport and an example of electrosensitization, IEEE Trans. Biomed. Eng. 63 (3) (2015) 571–580.

[48] Y. Mi, J. Xu, C. Yao, C. Li, H. Liu, Electroporation modeling of a single cell exposed to high-frequency nanosecond pulse bursts, IEEE Trans. Dielectr. Electr. Insul. 26 (2) (2019) 461–468.
[49] Y. Mi, J. Xu, Q. Liu, X. Wu, Q. Zhang, J. Tang, Single-cell electroporation with high-frequency nanosecond pulse bursts: Simulation considering the irreversible electroporation effect and experimental validation, Bioelectrochemistry 140 (2021), 107822.
[50] M. Pavlin, V. Leben, D. Miklavčič, Electroporation in dense cell suspension—Theoretical and experimental analysis of ion diffusion and cell permeabilization, Biochimica et Biophysica Acta (BBA)-General Subjects 1770 (1) (2007) 12–23.
[51] M. Pavlin, D. Miklavčič, Theoretical and experimental analysis of conductivity, ion diffusion and molecular transport during cell electroporation—relation between short-lived and long-lived pores, Bioelectrochemistry 74 (1) (2008) 38–46.
[52] M. Leguebe, A. Silve, L.M. Mir, C. Poignard, Conducting and permeable states of cell membrane submitted to high voltage pulses: mathematical and numerical studies validated by the experiments, J. Theor. Biol. 360 (2014) 83–94.
[53] J.-M. Escoffre, T. Portet, C. Favard, J. Teissié, D.S. Dean, M.-P. Rols, Electromediated formation of DNA complexes with cell membranes and its consequences for gene delivery, Biochimica et Biophysica Acta (BBA)-Biomembranes 1808 (6) (2011) 1538–1543.
[54] P.T. Vernier, Y. Sun, L. Marcu, S. Salemi, C.M. Craft, M.A. Gundersen, Calcium bursts induced by nanosecond electric pulses, Biochem. Biophys. Res. Commun. 310 (2) (2003) 286–295.
[55] A. Silve, A.G. Brunet, B. Al-Sakere, A. Ivorra, L.M. Mir, Comparison of the effects of the repetition rate between microsecond and nanosecond pulses: Electropermeabilization-induced electro-desensitization? Biochimica et Biophysica Acta (BBA)-General Subjects 1840 (7) (2014) 2139–2151.
[56] D. C. Sweeney, T. A. Douglas, and R. V. Davalos, "Characterization of cell membrane permeability in vitro part II: computational model of electroporation-mediated membrane transport," *Technology in cancer research & treatment*, vol. 17, p. 1533033818792490, 2018.
[57] D. C. Sweeney, J. C. Weaver, and R. V. Davalos, "Characterization of cell membrane permeability in vitro part I: transport behavior induced by single-pulse electric fields," *Technology in cancer research & treatment*, vol. 17, p. 1533033818792491, 2018.
[58] E. Neumann, E. Boldt, "Membrane electroporation: biophysical and biotechnical aspects", in *Charge and Field Effects in Biosystems—2*, Springer (1989) 373–382.
[59] R.A. Böckmann, B.L. De Groot, S. Kakorin, E. Neumann, H. Grubmüller, Kinetics, statistics, and energetics of lipid membrane electroporation studied by molecular dynamics simulations, Biophys. J . 95 (4) (2008) 1837–1850.
[60] V.F. Pastushenko, Y.A. Chizmadzhev, V.B. Arakelyan, Electric breakdown of bilayer lipid membranes: II. Calculation of the membrane lifetime in the steady-state diffusion approximation, J. Electroanal. Chem. Interfacial Electrochem. 104 (1979) 53–62.
[61] A. Barnett, J.C. Weaver, Electroporation: a unified, quantitative theory of reversible electrical breakdown and mechanical rupture in artificial planar bilayer membranes, Bioelectrochem. Bioenerg. 25 (2) (1991) 163–182.
[62] K.T. Powell, J.C. Weaver, Transient aqueous pores in bilayer membranes: a statistical theory, Bioelectrochem. Bioenerg. 15 (2) (1986) 211–227.
[63] J.C. Neu, W. Krassowska, Asymptotic model of electroporation, Phys. Rev. E 59 (3) (1999) 3471.
[64] J.T. Sengel, M.I. Wallace, Imaging the dynamics of individual electropores, Proc. Natl. Acad. Sci. 113 (19) (2016) 5281–5286.
[65] M.L. Fernández, M. Risk, R. Reigada, P.T. Vernier, Size-controlled nanopores in lipid membranes with stabilizing electric fields, Biochem. Biophys. Res. Commun. 423 (2) (2012) 325–330.
[66] M. Casciola, M.A. Kasimova, L. Rems, S. Zullino, F. Apollonio, M. Tarek, Properties of lipid electropores I: Molecular dynamics simulations of stabilized pores by constant charge imbalance, Bioelectrochemistry 109 (2016) 108–116.
[67] W. Krassowska, P.D. Filev, Modeling electroporation in a single cell, Biophys. J . 92 (2) (2007) 404–417.
[68] J.C. Weaver, Y.A. Chizmadzhev, Theory of electroporation: a review, Bioelectrochem. Bioenerg. 41 (2) (1996) 135–160.
[69] E.B. Sözer, C.F. Pocetti, P.T. Vernier, Asymmetric patterns of small molecule transport after nanosecond and microsecond Electropermeabilization, The Journal of membrane biology 251 (2) (2018) 197–210.
[70] C.S. Djuzenova, U. Zimmermann, H. Frank, V.L. Sukhorukov, E. Richter, G. Fuhr, Effect of medium conductivity and composition on the uptake of propidium iodide into electropermeabilized myeloma cells, Biochimica et Biophysica Acta (BBA)-Biomembranes 1284 (2) (1996) 143–152.
[71] V.L. Sukhorukov, C.S. Djuzenova, H. Frank, W.M. Arnold, U. Zimmermann, Electropermeabilization and fluorescent tracer exchange: The role of whole-cell capacitance, Cytometry: The Journal of the International Society for Analytical Cytology 21 (3) (1995) 230–240.
[72] W.D. Wilson, C.R. Krishnamoorthy, Y.-H. Wang, J.C. Smith, Mechanism of intercalation: ion effects on the equilibrium and kinetic constants for the interaction of propidium and ethidium with DNA, Biopolymers: Original Research on Biomolecules 24 (10) (1985) 1941–1961.
[73] Z. Vasilkoski, A.T. Esser, T.R. Gowrishankar, J.C. Weaver, Membrane electroporation: The absolute rate equation and nanosecond time scale pore creation, Phys. Rev. E 74 (2) (2006), 021904.
[74] C.L. Ting, N. Awasthi, M. Müller, J.S. Hub, Metastable prepores in tension-free lipid bilayers, Phys. Rev. Lett. 120 (12) (2018), 128103.
[75] E.B. Sözer, S. Haldar, P.S. Blank, F. Castellani, P.T. Vernier, J. Zimmerberg, Dye transport through bilayers agrees with lipid electropore molecular dynamics, Biophys. J . 119 (9) (2020) 1724–1734.
[76] J.T. Sengel, M.I. Wallace, Measuring the potential energy barrier to lipid bilayer electroporation, Philosophical Transactions of the Royal Society B: Biological Sciences 372 (1726) (2017) 20160227.
[77] M. Maccarrone, N. Rosato, A.F. Agrò, Electroporation enhances cell membrane peroxidation and luminescence, Biochem. Biophys. Res. Commun. 206 (1) (1995) 238–245.
[78] M. Breton, L.M. Mir, Investigation of the chemical mechanisms involved in the electropulsation of membranes at the molecular level, Bioelectrochemistry 119 (2018) 76–83.
[79] D. Wiczew, N. Szulc, M. Tarek, Molecular dynamics simulations of the effects of lipid oxidation on the permeability of cell membranes, Bioelectrochemistry 141 (2021), 107869.
[80] P. Boonnoy, V. Jarerattanachat, M. Karttunen, J. Wong-Ekkabut, Bilayer deformation, pores, and micellation induced by oxidized lipids, The journal of physical chemistry letters 6 (24) (2015) 4884–4888.
[81] K. Hristov, U. Mangalanathan, M. Casciola, O.N. Pakhomova, A.G. Pakhomov, Expression of voltage-gated calcium channels augments cell susceptibility to membrane disruption by nanosecond pulsed electric field, Biochimica et Biophysica Acta (BBA)-Biomembranes 1860 (11) (2018) 2175–2183.
[82] L. Rems, M.A. Kasimova, I. Testa, L. Delemotte, Pulsed electric fields can create pores in the voltage sensors of voltage-gated ion channels, Biophys. J . 119 (1) (2020) 190–205.
[83] A. Muralidharan, L. Rems, M.T. Kreutzer, P.E. Boukany, Actin networks regulate the cell membrane permeability during electroporation, Biochimica et Biophysica Acta (BBA)-Biomembranes 1863 (1) (2021), 183468.
[84] D.L. Perrier, et al., Response of an actin network in vesicles under electric pulses, Sci. Rep. 9 (1) (2019) 1–11.
[85] P.M. Graybill, R.V. Davalos, Cytoskeletal disruption after electroporation and its significance to pulsed electric field therapies, Cancers 12 (5) (2020) 1132.
[86] L. Rems, X. Tang, F. Zhao, S. Pérez-Conesa, I. Testa, and L. Delemotte, "Identification of electroporation sites in the complex lipid organization of the plasma membrane," *eLife*, vol. 11, p. e74773, Feb. 2022, doi: 10.7554/eLife.74773.
[87] I. van Uitert, S. Le Gac, A. van den Berg, The influence of different membrane components on the electrical stability of bilayer lipid membranes, Biochimica et Biophysica Acta (BBA)-Biomembranes 1798 (1) (2010) 21–31.
[88] T.B. Napotnik, T. Polajžer, D. Miklavčič, Cell death due to electroporation–A review, Bioelectrochemistry 141 (2021), 107871.
[89] M. Cemazar, G. Sersa, W. Frey, D. Miklavcic, J. Teissié, Recommendations and requirements for reporting on applications of electric pulse delivery for electroporation of biological samples, Bioelectrochemistry 122 (2018) 69–76.